

**Title** Rank-invariant Estimation of Inbreeding Coefficients.

**Authors** Qian S. Zhang  
Department of Biostatistics, University of Washington  
Seattle WA 98195-1617, USA

Jérôme Goudet  
Department of Ecology and Evolution, University of Lausanne  
CH-1015 Lausanne, Switzerland  
<https://orcid.org/0000-0002-5318-7607>

Bruce S. Weir  
Department of Biostatistics, University of Washington  
Seattle WA 98195-1617, USA  
<https://orcid.org/0000-0002-4883-1247>

**Corresponding Author** Bruce S. Weir  
Department of Biostatistics, University of Washington  
Seattle WA 98195-1617, USA  
Telephone: +1 (206) 221-7947; Fax: +1 (206) 543-3286  
Email: [bsweir@uw.edu](mailto:bsweir@uw.edu)

**Running Title** Estimation of Inbreeding Coefficients.

**Word Count** 6894 (Pages 3-19.)

# 1 ABSTRACT

2 The two alleles an individual carries at a locus are identical by descent (ibd) if they have descended  
3 from a single ancestral allele in a reference population, and the probability of such identity is the  
4 inbreeding coefficient of the individual. Inbreeding coefficients can be predicted from pedigrees  
5 with founders in the reference population, but estimation from genetic data is not possible unless  
6 data are available from the reference population. Published estimators, at best, estimate inbreeding  
7 coefficients relative to average ibd probabilities for some specified set of alleles. Estimators that  
8 make explicit use of sample allele frequencies as estimates of allele probabilities in the reference  
9 population have additional confounding when study individuals have different average kinships with  
10 the remaining individuals. This means that the ranking of those individual inbreeding coefficient  
11 estimates depends on the study sample and we show the variation in rankings for common estimators  
12 applied to 1000 Genomes data. Allele-sharing estimators of within-population inbreeding coefficients  
13 for a set of individuals, however, do have invariant rankings across all studies including those  
14 individuals. They are unbiased with a large number of SNPs. We discuss how allele sharing  
15 estimates of within-population inbreeding coefficients are the relevant quantities for a range of  
16 empirical applications.

17 **Keywords:** Estimation, F-statistics, Identity by descent, Inbreeding, Kinship, SNP data

# INTRODUCTION

Allelic dependence at a locus is usually quantified by inbreeding coefficients for individuals or populations, with these measures referring either to correlations of allelic state indicators (Wright 1922) or to probabilities of identity by descent, *ibd*, (Malécot 1948). In this paper we use *ibd* and we have advocated the use of allele-sharing estimators (Weir and Goudet 2017: WG17 henceforth, Goudet et al. 2018) that are unbiased for individual and population inbreeding coefficients relative to average kinships among specified pairs of individuals. Estimators, such as those in PLINK (Purcell et al. 2007) and GCTA (Yang et al. 2011), that use allele frequencies from a sample confound inbreeding estimates by the averages of individual kinships. Our work is also influenced by the need to estimate inbreeding coefficients from many millions of SNP genotypes where likelihood methods may not be feasible and instead we employ moment-based methods.

There have been many published accounts of inbreeding estimation, including the recent evaluation of several methods by Alemu et al. (2021) in this journal. Among those that refer to allele sharing, Li and Horvitz (1953) discussed an inbreeding estimator based on observed homozygosity, i.e. within-individual sharing of maternal and paternal alleles. They compared observed sharing to the value expected under zero inbreeding. They also constructed an estimator from the proportions of each allele type in a sample that were homozygous and gave an expression that was investigated further by Ritland (1996). Ritland used allele sharing within and between individuals in his work, and his inbreeding estimates assumed “independence or near-independence” between individuals. If individuals are not independent, then we show below that the rankings of his inbreeding coefficient estimates change with the sample. In WG17 we estimated inbreeding coefficients by comparing within-individual allele-sharing to average sharing between pairs of individuals in a sample. By not making explicit use of sample allele frequencies, we preserved the ranking of estimates across different samples and this will be a central theme of the present paper.

Ritland’s individual-level inbreeding coefficients were also derived Yang et al. (2011) as the correlation between uniting gametes and were expressed in terms of allele dosages for an individual and sample allele frequencies. This estimator was written as  $\hat{F}_{\text{UNI}}$  in Yengo et al. (2017), and is less biased than another estimator in Yang et al. (2011) obtained from the diagonal elements of a genomic relationship matrix (GRM) of VanRaden (2008). We compare these two estimates below with allele-sharing and other methods: pedigree-based path-counting (Wright 1922), maximum-likelihood (e.g. Hall et al. 2012) and runs of homozygosity (e.g. Ceballos et al. 2018).

# 49 METHODS

## 50 Statistical sampling

51 We can describe the dependence between pairs of uniting alleles with data from a single popula-  
52 tion without invoking an evolutionary model for the history of the population. In this “statisti-  
53 cal sampling” framework (Weir 1996) we do not consider the variation associated with stochastic  
54 evolutionary processes but we do consider the variation among samples from the same population.  
55 Although extensive sets of genetic data allow individual-level inbreeding coefficients to be estimated  
56 with high precision, we start with population-level estimation.

57 Allelic dependencies can be quantified with the usual within-population inbreeding coefficient,  
58 written here as  $f_W$  to emphasize it is a within-population quantity, defined by

$$H_l = 2p_l(1 - p_l)(1 - f_W) \quad (1)$$

59 where  $H_l$  is the population proportion of heterozygotes for the reference allele at SNP  $l$  and  $p_l$   
60 is the population proportion of that reference allele. The same value of  $f_W$  is assumed to apply  
61 for all SNPs. An immediate consequence of this definition is that the population proportions of  
62 homozygotes for the reference and alternative alleles are  $p_l^2 + p_l(1 - p_l)f_W$  and  $(1 - p_l)^2 + p_l(1 - p_l)f_W$   
63 respectively. This formulation allows  $f_W$  to be negative, and it is bounded below by the maximum  
64 of  $-p_l/(1 - p_l)$  and  $-(1 - p_l)/p_l$ . It is bounded above by 1. Hardy-Weinberg equilibrium, HWE,  
65 corresponds to  $f_W = 0$  and textbooks (e.g. Hedrick 2000) point out that negative values of  $f_W$   
66 indicate more heterozygotes than expected under HWE.

67 Observed heterozygote proportions  $\tilde{H}_l$  have  $H_l$  as within-population expectation  $\mathcal{E}_W$  over samples  
68 from the study population,  $\mathcal{E}_W(\tilde{H}_l) = H_l$ , and this would provide a simple estimator of  $f_W$  if the  
69 allele population proportions were known. In practice, however, these proportions are not known.  
70 Steele et al. (2014) suggested use of a database external to the study sample to provide reference  
71 allele proportions in forensic applications where a reference database is used for making inferences  
72 about the population relevant for a particular crime. The more usual approach is to use sample  
73 proportions  $\tilde{p}_l$  in the study sample in place of the true proportions  $p_l$  (equation 1 of Li and Horvitz,  
74 1953):

$$\hat{f}_{W_l} = 1 - \frac{\tilde{H}_l}{2\tilde{p}_l(1 - \tilde{p}_l)} \quad (2)$$

75 The moment estimator in Equation 2 is also an MLE of  $f_W$  when only one locus is considered, but

76 it is biased (Robertson and Hill 1984) since not only is it a ratio of statistics but also the expected  
 77 value  $\mathcal{E}_W[2\tilde{p}_l(1 - \tilde{p}_l)]$  over repeated samples of  $n$  randomly chosen individuals from the population  
 78 is  $2p_l(1 - p_l)[1 - (1 + f_W)/(2n)]$  (e.g. Weir 1996, p39).

79 This approach can be used to estimate the within-population inbreeding coefficient  $f_j$  for each  
 80 individual  $j$  in a sample from one population. These are the “simple” estimators of Hall et al.  
 81 (2017) and the  $\hat{f}_{\text{HOM}_j}$  of Yengo et al. (2017):

$$\hat{f}_{\text{HOM}_{jl}} = 1 - \frac{\tilde{H}_{jl}}{2\tilde{p}_l(1 - \tilde{p}_l)} \quad (3)$$

82 The sample heterozygosity indicator  $\tilde{H}_{jl}$  is one if individual  $j$  is heterozygous at SNP  $l$  and is zero  
 83 otherwise. Averaging Equation 3 over individuals gives the estimator based on SNP  $l$  in Equation 2  
 84 although it is the individual-specific values with which we are concerned in this paper.

85 A single SNP provides estimates that are either 1 or a negative value depending on  $\tilde{p}_l$ , so many  
 86 SNPs are used in practice. In both Hall et al. (2012) and Yengo et al. (2017) data were combined  
 87 over loci as weighted or “ratio of averages” estimators:

$$\hat{f}_{\text{Hom}_j} = 1 - \frac{\sum_l(\tilde{H}_{jl})}{\sum_l[2\tilde{p}_l(1 - \tilde{p}_l)]} \quad (4)$$

88 Gazal et al. (2014) referred to this estimator as  $f_{\text{PLINK}}$  as it is an option in PLINK. We show  
 89 below the generally good performance of this weighted estimator even though it is a function of  
 90 sample allele frequencies. We will consider throughout that a large number  $L$  of SNPs are used so  
 91 that ratios of sums of statistics over loci, such as in Equation 4, have expected values equal to the  
 92 ratio of expected values of their numerators and denominators. Ochoa and Storey (2021) showed  
 93 statistics of the form  $\tilde{A}_L/\tilde{B}_L$ , where  $\tilde{A}_L = \sum_{l=1}^L a_l/L$  and  $\tilde{B}_L = \sum_{l=1}^L b_l/L$ , have expected values  
 94 that converge almost surely to the ratio  $A/B$  when  $\mathcal{E}_W(\tilde{A}_L) = Ac_L$  and  $\mathcal{E}_W(\tilde{B}_L) = Bc_L$ . This result  
 95 requires  $|a_l|, |b_l|$  to both be no greater than some finite quantity  $C$ ,  $c_L$  to converge to a finite value  
 96  $c$  as  $L$  increases, and for  $Bc$  not to be zero. For the ratio in Equation 4,  $a_l = \tilde{H}_{jl}$ ,  $b_l = 2\tilde{p}_l(1 - \tilde{p}_l)$  so  
 97  $A = (1 - f_j)$ ,  $B = 1$  for large sample sizes  $n$ , and  $c_L = \sum_l 2p_l(1 - p_l)/L \leq 1/2$  so the conditions are  
 98 satisfied, providing at least one SNP is polymorphic. For an “average of ratios” estimator of the  
 99 form  $\sum_{l=1}^L (a_l/b_l)/L$ , the denominators  $b_l$  can be very small and convergence of its expected value  
 100 is not assured.

101 As an alternative to using sample allele frequencies, Hall et al. (2012) used maximum likelihood  
 102 to estimate population allele proportions for multiple loci whereas Ayres and Balding (1998) used  
 103 Markov chain Monte Carlo methods in a Bayesian approach that integrated out the allele proportion

104 parameters. Neither of those papers considered data of the size we now face in sequence-based  
 105 studies of many organisms, and we doubt the computational effort to estimate, or integrate over,  
 106 hundreds of millions of allele proportions in Equations 2 or 3 adds much value to inferences about  $f$ .  
 107 The allele-sharing estimators we describe in the next section regard allele probabilities as unknown  
 108 nuisance parameters and we show how to avoid estimating them or assigning them values.

109 Hall et al. (2012) used an EM algorithm to find MLEs for  $f_j$  when population allele proportions  
 110 were regarded as being known and equal to sample proportions. Alternatively, a grid search can be  
 111 conducted over the range of validity for the single parameter  $f_j$  that maximizes the log-likelihood

$$\ln[\text{Lik}(f_j)] = \text{Constant} + \sum_{l=1}^L \{ \tilde{H}_{jl} \ln[(1 - f_j)] + (1 - \tilde{H}_{jl}) \ln[1 - 2\tilde{p}_l(1 - \tilde{p}_l)(1 - f_j)] \} \quad (5)$$

112 Estimation of the within-population inbreeding coefficients  $f_W$  ( $F_{IS}$  of Wright 1922) and  $f_j$  does  
 113 not require any information beyond genotype proportions in samples from a study population, nor  
 114 does it make any assumptions about that population or the evolutionary forces that shaped the  
 115 population. The coefficients are simply measures of dependence of pairs of alleles within individuals.  
 116 We show in the next section that, in the absence of additional information, these coefficients also  
 117 govern the behavior of common published inbreeding estimators for the probability of alleles being  
 118 identical by descent.

## 119 Genetic Sampling

120 Inbreeding parameters of most interest in genetic studies are those that recognize the contribution  
 121 of previous generations to inbreeding in the present study population. This requires accounting  
 122 for “genetic sampling” (Weir 1996) between generations, thereby leading to an ibd interpretation  
 123 of inbreeding: ibd alleles descend from a single allele in a reference population. It also allows the  
 124 prediction of inbreeding coefficients by path counting when pedigrees are known (Wright 1922). If  
 125 individual  $J$  is ancestral to both individuals  $j'$  and  $j''$ , and if there are  $n$  individuals in the pedigree  
 126 path joining  $j'$  to  $j''$  through  $J$ , then  $F_j = \sum (0.5)^n (1 + F_J)$  where  $F_J$  is the inbreeding coefficient of  
 127 ancestor  $J$  and  $F_j$  is the inbreeding coefficient of offspring  $j$  of parents  $j'$  and  $j''$ . The sum is over  
 128 all ancestors  $J$  and all paths joining  $j'$  to  $j''$  through  $J$ . The expression is also the coancestry  $\theta_{j'j''}$   
 129 of  $j'$  and  $j''$ : the probability an allele drawn randomly from  $j'$  is ibd to an allele drawn randomly  
 130 from  $j''$ .

131 The allele proportion  $p_l$  in a study population has expectation  $\pi_l$  over evolutionary replicates of

132 the population from an ancestral reference population to the present time. Sample allele proportions  
 133  $\tilde{p}_l$  provide information about the population proportions  $p_l$ , and their statistical sampling properties  
 134 follow from the binomial distribution. We do not invoke a specific genetic sampling distribution for  
 135 the  $p_l$  about their expectations  $\pi_l$  although we do assume the second moments of that distribution  
 136 depend on probabilities of ibd for pairs of alleles. One consequence of the assumed moments is that  
 137 the probability of individual  $j$  in the study population being heterozygous, i.e. the total expected  
 138 value  $\mathcal{E}_T$  of the heterozygosity indicator over replicates of the history of that individual, is

$$\mathcal{E}_T(\tilde{H}_{j_i}) = 2\pi_l(1 - \pi_l)(1 - F_j) \quad (6)$$

139 The quantity  $F_j$  is the individual-specific version of  $F_{IT}$  of Wright (1922) and we can regard it as  
 140 the probability the two alleles at any locus for individual  $j$  are ibd. There is an implicit assumption  
 141 in Equation 6 that the reference population needed to define ibd is infinite and in HWE: there is  
 142 probability  $F_j$  that  $j$  has homologous alleles with a single ancestral allele in that population and  
 143 probability  $(1 - F_j)$  of  $j$  having homologous alleles with distinct ancestral alleles there. In the first  
 144 place, the single ancestral allele has probability  $\pi$  of being the reference allele for that locus and  
 145 the implicit assumption is that two ancestral alleles are both the reference type with probability  $\pi^2$ .  
 146 This does not mean there is an actual ancestral population with those properties, any more than  
 147 use of  $\mathcal{E}_T$  means there are actual replicates of the history of any population or individual, and we  
 148 note that Equation 6 does not allow higher heterozygosity than predicted by HWE. Nonetheless,  
 149 the concept of ibd allows theoretical constructions of great utility and we now present a framework  
 150 for approaching empirical situations.

151 Inbreeding, or ibd, implies a common ancestral origin for uniting alleles and statements about  
 152 sample allele proportions  $\tilde{p}_l$  require consideration of possible ibd for other pairs of alleles in the  
 153 sample. The total expectation of  $2\tilde{p}_l(1 - \tilde{p}_l)$  over samples from the population and over evolutionary  
 154 replicates of the study population is (Weir 1996, p176)

$$\mathcal{E}_T[2\tilde{p}_l(1 - \tilde{p}_l)] = 2\pi_l(1 - \pi_l) \left[ (1 - \theta_S) - \frac{1}{2n} (1 + F_W - 2\theta_S) \right] \quad (7)$$

155 where  $F_W$  is the average inbreeding coefficient in the sample,  $F_W = \sum_{j=1}^n F_j/n$ , and  $\theta_S$  is the  
 156 average coancestry in the sample,  $\theta_S = \sum_{j=1}^n \sum_{j' \neq j} \theta_{jj'} / [n(n - 1)]$ . Equivalent expressions were  
 157 given by McPeck et al. (2004) and DeGiorgio and Rosenberg (2008). We note the relationship  
 158  $f_W = (F_W - \theta_S)/(1 - \theta_S)$  given by Wright (1922) and we showed in WG17 the equivalent expression  
 159  $f_j = (F_j - \theta_S)/(1 - \theta_S)$  for individual-specific values ( $\theta_S$  is Wright's  $F_{ST}$ ).

160 For a large number of SNPs, the expectation of a ratio estimator of the type considered here is  
 161 the ratio of expectations (Ochoa and Storey 2021). Therefore, the total expectations of the  $\hat{f}_{\text{Hom}_j}$ ,  
 162 taking into account both statistical and genetic sampling, are

$$\mathcal{E}_T(\hat{f}_{\text{Hom}_j}) = 1 - \frac{1 - F_j}{(1 - \theta_S) - \frac{1}{2n}(1 + F_W - 2\theta_S)} = \frac{f_j - \frac{1}{2n}(1 + f_W)}{1 - \frac{1}{2n}(1 + f_W)} \quad (8)$$

163 For all sample sizes,  $\hat{f}_{\text{Hom}_j}$  has an expected value less than the true value  $f_j$ , with the bias being  
 164 of the order of  $1/n$ . The ranking of  $\mathcal{E}_T(\hat{f}_{\text{Hom}_j})$  values, however, is the same as the ranking of the  $f_j$   
 165 and, therefore, of the  $F_j$ . For large sample sizes, Equation 8 reduces to  $\mathcal{E}_T(\hat{f}_{\text{Hom}_j}) = f_j$ . Averaging  
 166 over individuals shows that  $\mathcal{E}_T(\hat{f}_{\text{Hom}}) = f_W$ : the population-level estimator in Equation 2 has total  
 167 expectation of  $f_W$ , not  $F_W$ .

168 A different outcome is found for the  $f_{\text{UNI}_j}$  estimator of Yengo et al. (2017) (i.e.  $\hat{f}^{III}$  of Yang  
 169 et al. 2011;  $f_{\text{GCTA3}}$  of Gazal et al. 2014). This estimator, with the weighted (w) ratio of averages  
 170 over loci we recommend, as opposed to the unweighted (u) average of ratios over loci used in their  
 171 papers, is

$$\hat{f}_{\text{UNI}_j}^w = \frac{\sum_{l=1}^L [X_{jl}^2 - (1 + 2\tilde{p}_l)X_{jl} + 2\tilde{p}_l^2]}{\sum_{l=1}^L 2\tilde{p}_l(1 - \tilde{p}_l)} \quad (9)$$

172 In this equation  $X_{jl}$  is the reference allele dosage, the number of copies of the reference allele, at  
 173 SNP  $l$  for individual  $j$ . It is equivalent to the estimator given by Ritland (1996, equation 5) and  
 174 attributed by him to Li and Horvitz (1953).

175 Ochoa and Storey (2021) showed that  $\hat{f}_{\text{UNI}_j}^w$  has expectation, for a large number of SNPs and a  
 176 large sample size, of

$$\mathcal{E}_T(\hat{f}_{\text{UNI}_j}^w) = \frac{F_j - 2\Psi_j + \theta_S}{1 - \theta_S} = f_j - 2\psi_j \quad (10)$$

177 where  $\Psi_j$  is the average coancestry of individual  $j$  with other members of the study sample:  $\Psi_j =$   
 178  $\sum_{j'=1, j' \neq j}^n \theta_{jj'} / (n - 1)$ . We term  $\psi_j = (\Psi_j - \theta_S) / (1 - \theta_S)$  the within-population individual-specific  
 179 average kinship coefficient. The  $\Psi_j$  have an average of  $\theta_S$  over members of the sample, so the  
 180 average of the  $\psi_j$ 's is zero and expected value of the average of the  $\hat{f}_{\text{UNI}_j}^w$  is  $f_W$ , as is the case for  
 181  $\hat{f}_{\text{AS}_j}$ .

182 Equation 10 shows that the  $\hat{f}_{\text{UNI}_j}^w$  have expected values with the same ranking as the  $F_j$  values  
 183 only if there is no kinship among pairs of individuals or if every individual  $j$  in the sample has the  
 184 same average kinship  $\psi_j$  with other sample members.



185 Finally, we mention another common estimator described by VanRaden (2008) and termed  
 186  $f_{\text{GCTA1}}$  by Gazal et al. (2014) and available from the GCTA software (Yang et al., 2011) with  
 187 option `--ibc`. We referred to this as the “standard” estimator in WG17. The weighted version for  
 188 multiple loci is

$$\hat{f}_{\text{STD}_j}^w = \frac{\sum_l (X_{jl} - 2\tilde{p}_l)^2}{\sum_l 2\tilde{p}_l(1 - \tilde{p}_l)} - 1 \quad (11)$$

189 and it has the large-sample expectation of  $(f_j - 4\psi_j)$  as is implied by Equation 13 of WG17 and  
 190 as was given by Ochoa and Storey (2021). We summarize the various measures of inbreeding and  
 191 coancestry in Table 1, and we include sample sizes in the expectations shown in Table 2.

## 192 Tables 1 and 2

193 The  $\hat{f}_{\text{HOM}}$ ,  $\hat{f}_{\text{UNI}}$ ,  $\hat{f}_{\text{STD}}$  and  $\hat{f}_{\text{MLE}}$  estimators of individual or population inbreeding coefficients  
 194 make explicit use of sample allele proportions. This means that all four have small-sample biases,  
 195 and none of the four provide estimates of the ibd quantities  $F$  or  $F_j$ . We showed that  $\hat{f}_{\text{HOM}}$  is  
 196 actually estimating the within-population inbreeding coefficients: the total inbreeding coefficients  
 197 *relative to* the average coancestry of pairs of individuals in the sample, but  $\hat{f}_{\text{UNI}}$  and  $\hat{f}_{\text{STD}}$  are  
 198 estimating expressions that also involve average kinships  $\psi$ .

## 199 Allele Sharing

200 In a genetic sampling framework, and with the ibd viewpoint, we consider within-individual allele  
 201 sharing proportions  $A_{jl}$  for SNP  $l$  in individual  $j$  (we used  $M$  rather than  $A$  in WG17 and in Goudet  
 202 et al. 2018). These equal one for homozygotes and zero for heterozygotes and sample values can  
 203 be expressed in terms of allele dosages,  $\tilde{A}_{jl} = (X_{jl} - 1)^2$ . We also consider between-individual  
 204 sharing proportions  $A_{jj'l}$  for SNP  $l$  and distinct individuals  $j$  and  $j'$ . These are equal to one for  
 205 both individuals being the same homozygote, zero for different homozygotes, and 0.5 otherwise.  
 206 Observed values can be written as  $\tilde{A}_{jj'l} = [1 + (X_{jl} - 1)(X_{j'l} - 1)]/2$ , with an average over all pairs  
 207 of distinct individuals in a sample of  $\tilde{A}_{sl}$ . Astle and Balding (2009) introduced  $\tilde{A}_{jj'l}$  as a measure  
 208 of identity in state of alleles chosen randomly from individuals  $j$  and  $j'$ , and Ochoa and Storey  
 209 (2021) used a simple transformation of this quantity. The allele sharing for an individual with itself  
 210 is  $A_{j jl} = (1 + A_{jl})/2$ .

211 The same logic that led to Equation 6 provides total expectations for allele-sharing proportions  
 212 for all  $j, j'$ :

$$\begin{aligned}\mathcal{E}_T(\tilde{A}_{jj'l}) &= 1 - 2\pi_l(1 - \pi_l)(1 - \theta_{jj'}) \\ \mathcal{E}_T(\tilde{A}_{Sl}) &= 1 - 2\pi_l(1 - \pi_l)(1 - \theta_S)\end{aligned}$$

213 Note that  $\theta_{jj} = (1 + F_j)/2$ . The nuisance parameter  $2\pi_l(1 - \pi_l)$  cancels out of the ratio  $\mathcal{E}_T(\tilde{A}_{jj'l} -$   
 214  $\tilde{A}_{Sl})/\mathcal{E}_T(1 - \tilde{A}_{Sl})$  and this motivates definitions of allele-sharing estimators of the inbreeding coef-  
 215 ficient for individual  $j$  and the kinship coefficient for individuals  $j, j'$  as

$$\hat{f}_{AS_j} = \frac{\sum_l(\tilde{A}_{jl} - \tilde{A}_{Sl})}{\sum_l(1 - \tilde{A}_{Sl})}, \quad \hat{\psi}_{AS_{jj'}} = \frac{\sum_l(\tilde{A}_{jj'l} - \tilde{A}_{Sl})}{\sum_l(1 - \tilde{A}_{Sl})} \quad (12)$$

216 For a large number of SNPs, these are unbiased for  $f_j$  and  $\psi_{jj'}$  for all sample sizes. We show below  
 217 the satisfactory behavior of  $\hat{f}_{AS_j}$  for simulated data, and consistency of rankings over different  
 218 sampling frames, such as population, ancestry group or whole world for the 1000 Genomes data  
 219 (The 1000 Genomes Project Consortium 2015). We showed in WG17 there is no need to filter on  
 220 minor allele frequency to preserve the lack of bias.

221 For large sample sizes,  $(1 - \tilde{A}_{Sl}) \approx 2\tilde{p}_l(1 - \tilde{p}_l)$ . Under that approximation,  $\hat{f}_{AS_j}$  is the same  
 222 as  $\hat{f}_{Hom_j}$  but the approximation is not necessary in computer-based analyses. Summing the large-  
 223 sample estimates over individuals not equal to  $j$  gives an estimator for the average individual kinship  
 224  $\psi_j$ :

$$\hat{\psi}_{AS_j} = -\frac{\sum_l(X_{jl} - 2\tilde{p}_l)(1 - 2\tilde{p}_l)}{\sum_l 4\tilde{p}_l(1 - \tilde{p}_l)} \quad (13)$$

225 Adding  $2\hat{\psi}_{AS_j}$  to  $\hat{f}_{UNL_j}^w$  gives  $\hat{f}_{AS_j}$ , as expected, as does adding  $4\hat{\psi}_{AS_j}$  to  $\hat{f}_{STD_j}^w$ . Similarly,  $\hat{\psi}_{AS_{jj'}}$  is  
 226 obtained by adding  $\hat{\psi}_{AS_j}$  and  $\hat{\psi}_{AS_{j'}}$  to  $\hat{\psi}_{STD_{jj'}}$ , where (Yang et al. 2011)

$$\hat{\psi}_{STD_{jj'}} = \frac{\sum_l(X_{jl} - 2\tilde{p}_l)(X_{j'l} - 2\tilde{p}_l)}{\sum_l 4\tilde{p}_l(1 - \tilde{p}_l)}$$

227 These are the elements of the first method for constructing the GRM given by VanRaden (2008).

228 When inbreeding and coancestry coefficients are defined as ibd probabilities they are non-  
 229 negative, but the within-population values  $f$  and  $\psi$  will be negative for individuals, or pairs of  
 230 individuals, having smaller ibd allele probabilities than do pairs of individuals in the sample, on  
 231 average. Individual-specific values of  $f$  always have the same ranking as the individual-specific  
 232  $F$  values, and they are estimable. Negative estimates can be avoided by the transformation to

233  $(\hat{f}_{AS_j} - \hat{f}_{AS_j}^{\min}) / (1 - \hat{f}_{AS_j}^{\min})$  where  $\hat{f}_{AS_j}^{\min}$  is the smallest value over individuals of the  $\hat{f}_{AS_j}$ 's. We don't  
234 see the need for this transformation, and we noted above the recognition of the utility of negative  
235 values. Ochoa and Storey (2021) wished to estimate  $F_j$  rather than  $f_j$  and, to overcome the lack of  
236 information about the ancestral population serving as a reference point for ibd, they assumed the  
237 least related pair of individuals in a sample have a coancestry of zero. We showed in WG17 that  
238 this brings estimates in line with path-counting predicted values when founders are assumed to be  
239 not inbred and unrelated, but we prefer to avoid the assumption. We stress that, absent external  
240 information or assumptions,  $F$  is not estimable. Instead, linear functions of  $F$  that describe ibd of  
241 target pairs of alleles relative to ibd in a specified set of alleles are estimable and have utility in  
242 empirical studies.

## 243 **Runs of Homozygosity**

244 Each of the inbreeding estimators considered so far has been constructed for individual SNPs and  
245 then combined over SNPs. Observed values of allelic state are used to make inferences about the  
246 unobserved state of identity by descent. Estimators based on runs of homozygosity (ROH), however,  
247 suppose that ibd for a region of the genome can be observed. Although  $F$  is the probability an  
248 individual has ibd alleles at any single SNP, in fact ibd occurs in blocks within which there has  
249 been no recombination in the paths of descent from common ancestor to the individual's parents.  
250 Whereas a single SNP can be homozygous without the two alleles being ibd, if many adjacent  
251 SNPs are homozygous the most likely explanation is that they are in a block of ibd (Gibson et  
252 al. 2006). There can be exceptions, from mutation for example, and several publications give  
253 strategies for identifying runs of homozygotes for which ibd may be assumed (e.g. Gazal et al.  
254 2014, Joshi et al. 2015). These strategies include adjusting the size of the blocks, the numbers of  
255 heterozygotes or missing values allowed per block, the minor allele frequency, and so on. These  
256 software parameters affect the size of the estimates (Meyermans et al. 2020). More sophisticated  
257 methods (e.g. Narasimhan et al. 2016) use hidden Markov models where ibd is the hidden status  
258 of an observed homozygote. This model-based approach necessarily has assumptions, such as HWE  
259 in the sampled population.

260 We provide more details elsewhere, but we note here that ROH methods offer a useful alternative  
261 to SNP-by-SNP methods even though they cannot completely compensate for lack of information  
262 on the ibd reference population. We note also that shorter runs of ibd result from more distant

263 relatedness of an individual’s parents, so that ROH procedures can be set to distinguish recent  
264 (familial) ibd from distant (evolutionary) ibd. SNP-by-SNP estimators do not make a distinction  
265 between these two time scales.

## 266 **Simulation Study**

267 We generated a founder set of 50 founder individuals with 20,000 SNPs over a 20 Morgan map  
268 by using the mspms program (Kelleher et al. 2016). We then used quantiNemo software (Neuen-  
269 schwander et al. 2019) to simulate a five-generation pedigree of hermaphroditic individuals mating  
270 randomly, excluding selfing, with each mating producing a number of offspring drawn from a Poisson  
271 distribution with mean two. The zero-th generation was the 50 founders, the first generation had  
272 47 individuals and the second, third, fourth and fifth generations had 58, 56, 57 and 65 individuals  
273 respectively. We followed the founder gametes through the pedigree using a custom R script and  
274 allowing for recombination based on the 20 Morgan genetic map.

275 Each of the 100 alleles per SNP among the founders was given a unique identifier so that alleles  
276 in subsequent generations with the same identifier had actual identity by descent relative to the  
277 founders. The average actual ibd proportions over loci, within individuals and between each pair  
278 of individuals, provided “gold standard” inbreeding and coancestry coefficients, as opposed to the  
279 pedigree-based values we calculated by path counting.

280 The pedigree was constructed to provide fairly high levels of predicted coancestry among pairs  
281 of the 283 non-founder individuals, ranging from zero to 0.464, with a mean of  $\theta_S = 0.053$ , assuming  
282 the 50 founders were unrelated and not inbred. The pedigree inbreeding coefficients ranged from  
283 zero to 0.367, with a mean of  $F_W = 0.050$ . The within-population inbreeding coefficient for the  
284 set of 283 non-founder individuals is  $f = (F_W - \theta_S)/(1 - \theta_S) = 0.003$ . Note, however, that the  
285 50 individuals regarded as founders for the subsequent 283 had their own joint histories from the  
286 mspms simulation. These 50 had an average within-individual allele sharing of  $\tilde{A}_W = 0.80385$  and an  
287 average between-individual allele sharing of  $\tilde{A}_S = 0.80355$ . The difference of these two proportions,  
288 which would be zero for a reference set of non-inbred and unrelated individuals, provides a within-  
289 founder allele-sharing inbreeding coefficient  $\hat{f}_W$  of 0.0015.

290 The various estimators of inbreeding examined with these data are shown in Table 2, and the  
291 correlation coefficients for each pair of estimates over the whole set of 283 non-founder individuals  
292 are shown in Table 3. There are very high correlations between pedigree and gold-standard values

293 and also very high correlations between  $\hat{f}_{\text{HOM}}$  and  $\hat{f}_{\text{AS}}$  values, both as expected. In populations  
 294 without substructure, random mating would lead to similar values for inbreeding and coancestry  
 295 levels, so  $\hat{f}_{\text{AS}}$  and  $\hat{\psi}_{\text{AS}}$  values would have similar values. There are lower correlations of  $\hat{f}_{\text{UNI}}$  and  
 296  $\hat{f}_{\text{STD}}$  with pedigree-based or gold-standard inbreeding coefficients since those estimates reflect both  
 297  $f$  and  $\psi$ .

298 We see in Table 3 that  $\hat{F}_{\text{ROH}}$  values are the most highly correlated with  $F_{\text{Gold}}$ : this high correla-  
 299 tion was obtained by adjusting the block size (100 SNPs) and the block overlap amount (50 SNPs)  
 300 to bring estimates close to the known  $F_{\text{Gold}}$  values. In practice the  $F_{\text{Gold}}$  values are not known and  
 301 the other estimators are all evaluated without external information. The high correlation of  $\hat{f}_{\text{AS}}$   
 302 and maximum likelihood values shows that  $\hat{f}_{\text{MLE}}$  is estimating  $f$  rather than  $F$  because it uses the  
 303 sample allele frequencies in place of the unknown allele probabilities. The weighted and unweighted  
 304 versions of  $\hat{f}_{\text{UNI}}$  are highly correlated with each other and with their gold values, but this is not the  
 305 case for  $\hat{f}_{\text{STD}}$ .

306 **Table 3**

307 Figure 1 (left) illustrates the linear relationship between  $f_{\text{Ped}_j}$  and  $F_{\text{Ped}_j}$ :  $f_{\text{Ped}_j} = (F_{\text{Ped}_j} -$   
 308  $\theta_{\text{Ped}_S}) / (1 - \theta_{\text{Ped}_S})$  where  $\theta_{\text{Ped}_S} = 0.053$  is the average coancestry of pairs of non-founders, also  
 309 calculated from the pedigree. The  $F_{\text{Gold}_j}$  and  $f_{\text{Gold}_j}$  values are highly, and equally, correlated with  
 310 the corresponding pedigree values, as is shown for  $f_{\text{Gold}_j}$  in Figure 1 (center). The variation we see  
 311 in Figure 1 (center) for  $f_{\text{Gold}_j}$  around  $F_{\text{Ped}_j}$  reflects the relatively small number of 20K SNPs and  
 312 the relatively small map length spanned by these SNPs. We have previously (Hill and Weir 2011)  
 313 pointed out the variation of actual inbreeding about expected values, even for whole genomes, and  
 314 Wang (2016) showed that the number of SNPs also has an effect. The expected lack of relationship  
 315 between pedigree-based values of individual average coancestry  $\psi_j$  and individual inbreeding  $f_j$ ,  
 316 leading to variable rankings for some estimators based on sample allele frequencies, is shown in  
 317 Figure 1 (right).

318 **Figure 1**

319 Figure 2 (left) illustrates the similarity of  $\hat{F}_{\text{ROH}}$  and  $F_{\text{Gold}}$  and Figure 2 (center) shows good  
 320 agreement between  $\hat{F}_{\text{ROH}}$  and  $\hat{f}_{\text{AS}}$ . Figure 2 (right) shows the low bias of the allele-sharing estimators  
 321  $\hat{f}_{\text{AS}_j}$  for the gold-standard within-population inbreeding coefficients  $f_{\text{Gold}_j}$ . Figure 3 shows  $\hat{f}_{\text{UNI}_j}$  to

322 be a better estimator of  $f_{\text{Gold}_j}$  than is  $\hat{f}_{\text{STD}_j}$ , as noted by Yang et al. (2011), and better performance  
323 for the weighted than unweighted averages over SNPs.

## 324 **Figures 2 and 3**

### 325 **1000 Genomes Data**

326 We used 77m SNPs from the 22 autosomes for the 26 populations of the 1000 Genomes whole genome  
327 data to estimate inbreeding coefficients for all 2504 individuals in the project. Our focus was on the  
328 invariance of estimate rankings as the reference set of individuals changed from the population from  
329 which each individual was sampled, to the continental group for that population, to the whole world.  
330 We calculated the estimates  $\hat{f}_{\text{AS}_j}$  and  $\hat{f}_{\text{UNI}_j}^u$  for each individual and each reference set, and ranked  
331 estimates within each population. The two sets of estimates for all individuals are shown separately  
332 in Figure 4. Figures S1 and S2 show  $\hat{f}_{\text{UNI}_j}^u$  versus  $\hat{f}_{\text{AS}_j}$  for estimates and ranks respectively.

## 333 **Figure 4**

334 Figure 4 shows that within-population inbreeding coefficients  $\hat{f}_{\text{AS}}$  for all 1000 Genomes popu-  
335 lations (except the AMR group: CLM, MXL, PEL, PUR) are essentially the same, and generally  
336 close to zero, when they are estimated relative to average coancestry within each population or  
337 continental group but change when the complete set of 26 populations is used as a reference. These  
338 latter values compare the allele sharing for each individual to the same reference value, the average  
339 sharing over all pairs of individuals in the whole dataset. The world reference shows markedly differ-  
340 ent  $\hat{f}_{\text{AS}}$  values for the African populations (AFR), reflecting their higher levels of genetic diversity.  
341 The rankings for  $\hat{f}_{\text{AS}}$  within a population, by construction, do not change with reference set. There  
342 are some high value outliers when the world is used as a reference: four of the five highest values  
343 are from AMR/PEL. These high  $\hat{f}_{\text{AS}}$  values reflect admixture, consanguineous matings and high  
344 evolutionary coancestry. On the other hand, the  $\hat{f}_{\text{UNI}}$  values are higher for African individuals than  
345 for any other individuals when the allele frequencies are from all 26 populations: this reflects an  
346 African-specific pattern of negative average individual kinships  $\psi$ , rather than higher values of the  
347 inbreeding coefficients  $F$ .

348 The critical role that average kinship plays in inbreeding estimation is illustrated in Figure 5.  
349 With the world as reference set, the allele-sharing inbreeding estimates  $\hat{f}_{\text{AS}}$  are tightly clustered  
350 for European (EUR) individuals, a little more diverse for East Asian (EAS) individuals, much

351 more diverse for South Asian (SAS) and African (AFR) individuals, and substantially diverse for  
352 American (AMR) individuals. These values are consistent with those reported for the numbers of  
353 variant sites per genome (The 1000 Genomes Project Consortium, 2015). The variation among  
354 African and American average kinships  $\hat{\psi}_{AS}$  is substantial: as these quantities determine how the  
355 expected values of  $\hat{F}_{UNI}$  and  $\hat{F}_{STD}$  differ from the  $f$  target parameters, it is clear that these estimates  
356 cannot be used to rank individuals by their inbreeding levels.

### 357 **Figure 5**

358 For the African population ASW, individual NA20294 has  $\hat{f}_{AS}$  values of  $-0.009, 0.001, -0.130$   
359 using ASW, AFR or World as a reference set and each estimate is ranked as number 16 among the  
360 61 ASW estimates. The same individual has  $\hat{f}_{UNI}^u$  values of  $-0.007$  (rank 36),  $0.001$  (rank 16) and  
361  $0.028$  (rank 60) using ASW, AFR or World allele frequencies. Estimator  $\hat{f}_{UNI}^u$  indicates NA20294  
362 to be among the least inbred of the ASW individuals when AFR sample allele frequencies are used,  
363 but among the most inbred when world-wide sample allele frequencies are used, even though the  
364 individual's own genotype is the same for each analysis. Other examples of rankings changing with  
365 reference population for  $\hat{f}_{UNI}$  are shown in Figure S3. This can have implications for studies of  
366 inbreeding depression, where trait values are regressed on estimated inbreeding coefficients.

367 A comparison of runs-of-homozygosity estimates  $\hat{F}_{ROH_j}$  with SNP-by-SNP estimates is shown in  
368 Figure 6. The ROH estimates were produced with the `--homozyg --homozyg-snp2 --homozyg-kb100`  
369 options in PLINK (Meyermans et al. 2020). The values of  $\hat{F}_{ROH_j}$  depend on the PLINK settings  
370 for minor allele frequency pruning and linkage disequilibrium pruning, as well as on SNP density, so  
371 their expected values may differ from the true  $F_j$  values. The left panel shows  $\hat{f}_{AS_j}$  values and these  
372 have a correlation of 0.998 with  $\hat{F}_{ROH_j}$ . The right panel shows  $\hat{f}_{UNI_j}$  estimates and these appear to  
373 have little relationship with  $\hat{F}_{ROH_j}$ .

### 374 **Figure 6**

375 Narasimhan et al. (2016) used a hidden Markov model for obtaining  $\hat{f}_{ROH_j}$  values (Figure  
376 S4). There is very good agreement with  $\hat{f}_{AS_j}$  values, providing the admixed AMR populations are  
377 not used. Gazal et al. (2015) also used a hidden Markov model to obtain inbreeding estimates,  
378 although their method requires sample allele frequencies and so may have estimates of  $F$  confounded  
379 by average individual-specific average kinships. However, there is good agreement of  $\hat{f}_{AS_j}$  values  
380 with the values given by Gazal et al. (Figure S5).

## 381 DISCUSSION

382 Discussions on the estimation of individual inbreeding coefficients generally refer to  $F$ , the prob-  
383 ability an individual has pairs of homologous alleles that are identical by descent. Among the  
384 estimators we have considered here,  $\hat{F}_{\text{ROH}}$  addresses  $F$  by assuming that long runs of homozygous  
385 SNPs represent ibd regions. The ROH estimates, however, are conditional on the settings used  
386 to calculate the estimates, and actual ibd in short runs of homozygotes may be ignored, so the  
387 expected values of these estimators is not known. The Bayesian approach of Vogl et al. (2002) also  
388 addresses  $F$  but at the computational cost of estimating allele proportions in a reference popula-  
389 tion assumed to have zero inbreeding or relatedness. All the other estimators considered here are,  
390 instead, addressing the within-population inbreeding coefficient  $f$  that compares  $F$  values to ibd  
391 probabilities for pairs of individuals. There is no need to specify the reference population implicit in  
392 the definition of identity by descent. There is also no need to assume the particular individuals in a  
393 sample have an inbreeding coefficient of zero. For large numbers of SNPs, allele-sharing estimators  
394  $\hat{f}_{\text{AS}}$  are unbiased for  $f$  for all sample sizes and have values for a set of individuals that have invariant  
395 ranks over studies that include that set. We show that estimators using sample allele frequencies  
396 are estimating some combination of  $f$  and of individual-specific average kinships  $\psi$  with individuals  
397 in the study. Estimators with expectations depending on  $\psi$  do not have invariant rankings, as we  
398 showed with data from the 1000 Genomes project as the study scope varied from the population to  
399 the continent to the world.

400 Our ibd-based model rests on expectations of allele-sharing proportions satisfying expressions  
401 such as Equation 6. There is no requirement for non-overlapping generations, or homogeneous  
402 populations, for example. This generality is a consequence of not needing allele frequencies, whether  
403 these refer to a population or to an individual.

404 The role of ibd probabilities in theoretical population and quantitative genetic contexts is well  
405 known, but we suggest it is rank-invariant estimators for the within-population parameters  $f_j$  that  
406 are of relevance for empirical studies and we offer the examples in the following sections.

### 407 Genotype Probabilities

408 There is often a need to estimate genotype probabilities from observed allele proportions using  
409 formulations with allele probabilities and ibd probabilities  $F$  (e.g. National Research Council 1996  
410 for forensic science). Following Equation 7 we see that it is  $2\tilde{p}_l(1 - \tilde{p}_l)(1 - f_j)$  rather than  $2\tilde{p}_l(1 -$



411  $\tilde{p}_l)(1 - F_j)$  that is unbiased for  $2\pi_l(1 - \pi_l)(1 - F_j)$  if  $F_j$  and  $f_j$  are known.

## 412 Inbreeding Depression

413 Inbreeding is known to affect, linearly, the expected value of quantitative traits, and studies of  
414 inbreeding depression often proceed by regressing trait means on inbreeding levels. In Yengo et al.  
415 (2017), we used  $\hat{F}_{\text{ROH}}$ ,  $\hat{f}_{\text{HOM}}$  and  $\hat{f}_{\text{UNI}}$  as inbreeding estimates. Kardos et al. (2018) pointed out that  
416 we did not discuss the distinction between  $F$  and  $f$ . We responded (Yengo et al. 2018) with reasons  
417 for not wishing to use  $\hat{F}_{\text{ROH}}$  and we could have pointed out the linear relationship between  $f_j$  and  $F_j$   
418 and the high correlation we showed above between  $\hat{f}_{\text{AS}_j}$  and  $\hat{F}_{\text{ROH}_j}$  means that regressing on either  
419  $\hat{F}_{\text{ROH}}$  or  $\hat{f}_{\text{AS}}$  should lead to similar results. A SNP with highly significant inbreeding depression  
420 revealed by regressing trait values on  $\hat{F}_{\text{ROH}}$  should also be highly significant when regressing on  $\hat{f}_{\text{AS}_j}$ .  
421 In less-homogeneous populations than represented by the UK Biobank data (Allen et al. 2012) we  
422 used in Yengo et al. (2017), it would appear to be better to use  $\hat{f}_{\text{AS}_j}$  than  $\hat{f}_{\text{UNI}_j}$  to avoid any effects  
423 of individual-specific average kinships on inbreeding estimates. Alemu et al. (2021) pointed out  
424 that  $\hat{f}_{\text{HOM}}$  (and  $\hat{f}_{\text{AS}}$ ), gives equal weights to all SNPs, whereas  $\hat{f}_{\text{UNI}}$  gives greater weight to SNPs  
425 with rare alleles. Alemu et al. did not consider the role of individual average kinships in the bias  
426 of  $\hat{f}_{\text{UNI}}$ .

## 427 Genetic Relatedness Matrix

428 Inbreeding is also known to affect, linearly, the additive component of genetic variance. For ad-  
429 ditive traits, the genetic variance for individual  $j$  is  $(1 + F_j)\sigma_A^2$  where  $\sigma_A^2$  is the additive variance  
430 for populations in Hardy-Weinberg equilibrium. Consequently, the expected value of the sample  
431 variance  $\tilde{V}_T$  of trait values over a sample of  $n$  individuals is (Speed et al. 2012)

$$\mathcal{E}_T(\tilde{V}_T) = \frac{1}{n} \left( \text{tr}(\mathbf{G}) - \frac{1}{n-1} \Sigma_{\mathbf{G}} \right) \sigma_A^2 + \sigma_e^2$$

432 Here the trait is additive and the errors, with variance  $\sigma_e^2$ , are independent of genetic effects. The  
433 GRM  $\mathbf{G}$  has trace  $\text{tr}(\mathbf{G})$  and sum of off-diagonal elements  $\Sigma_{\mathbf{G}}$ . If the GRM elements are  $(1 + F_j)$   
434 on the diagonal and  $2\theta_{jj'}$  off the diagonal then the trace is  $n(1 + F_W)$  and the sum of off-diagonal  
435 elements is  $n(n-1)\theta_S$  so the genetic component of  $V_T$  is  $(1 + F_W - 2\theta_S)\sigma_A^2$ . If the GRM is replaced  
436 by a matrix with allele-sharing inbreeding and kinship estimates, this becomes  $(1 + f_W)\sigma_A^2$ , reflecting

437 that it is the within-population estimated GRM that is used in practice. We show elsewhere that  
438 the same expected variance holds with GRMs constructed with  $\hat{f}_{\text{STD}}$  or  $\hat{f}_{\text{UNI}}$ .

439 In summary, we have shown that inbreeding measures of utility in empirical studies are “within-  
440 population” with the choice of population being at the discretion of the investigator. With allele-  
441 sharing inbreeding estimators, the population specifies the set of individuals whose pairwise coances-  
442 try is the reference against which inbreeding is measured. For estimators making explicit use of  
443 sample allele frequencies, it is the population that furnishes those frequencies, although then in-  
444 breeding estimates are confounded by individual-specific average kinships. We showed algebraically  
445 and empirically that allele-sharing estimators have invariant rankings across choice of population.

## 446 SOFTWARE

447 Estimation of inbreeding coefficients can be performed with the following software.

448  $\hat{F}_{\text{HOM}}$ : PLINK

449  $\hat{F}_{\text{Uni}}$ : PLINK2, GCTA.

450  $\hat{F}_{\text{Std}}$ : PLINK1, GCTA.

451  $\hat{F}_{\text{ROH}}$ : PLINK1, BCFtools/ROH, FSuite.

452  $\hat{F}_{\text{AS}}$ : SNPRelate, hierFstat.

453  $\hat{F}_{\text{MLE}}$ : SNPRelate.

454 Software is available at:

455 BCFtools/ROH: <https://samtools.github.io/bcftools/howtos/roh-calling.html>

456 FSuite: <http://genestat.cephb.fr/software/index.php/FSuite>

457 GCTA: <http://gump.qimr.edu.au/gcta>

458 hierFstat: <https://cran.r-project.org/web/packages/hierfstat/index.html>

459 PLINK: <http://pngu.mgh.harvard.edu/purcell/plink/>

460 PLINK2: <https://www.cog-genomics.org/plink/2.0/>

461 SNPRelate: <http://www.bioconductor.org/packages/release/bioc/html/SNPRelate.html>

462

## 463 DATA ARCHIVING

464 The simulated data are available as an online supplement.

465 The 1000 Genomes data are available at <ftp://ftp.1000genomes.ebi.ac.uk/vol1/ftp/>.

## 466 CONFLICT OF INTEREST

467 The authors declare no conflicts of interest.

## 468 ACKNOWLEDGMENTS

469 This work was supported in part by Grants 31003A-138180 and IZKOZ3-157867 from the Swiss

470 National Science Foundation, and by Grants GM081062 and GM075091 from the US National

471 Institutes of Health. We are grateful for the comments of reviewers and editors on an earlier version  
472 of this paper.

473

474 Allen N, et al. (2012). UK Biobank: Current status and what it means for epidemiology. *Health  
475 Policy Technol* 1:123126.

476

477 Alemu AW, Kadir NK, Harland C, Paux P, Charlier C, Caballero A, Druet T (2021). An evaluation  
478 of inbreeding measures using a whole-genome sequenced cattle pedigree. *Heredity* 126:410-423.  
479

480 Astle W, Balding DJ (2009). Population structure and cryptic relatedness in genetic association  
481 studies. *Stat Sci* 24:451-471.  
482

483 Ayres KL, Balding DJ (1998). Measuring departures from Hardy-Weinberg: a Markov chain Monte  
484 Carlo method for estimating the inbreeding coefficient. *Heredity* 80:769-777.  
485

486 Ceballos FC, Joshi PK, Clark DW, Ramsay M, Wilson JF (2018). Runs of homozygosity: windows  
487 into population history and trait architecture. *Nature Reviews Genetics* 19: 220234.  
488

489 Chang CC, Chow CC, Tellier LCAM, Vattikuti S, Purcell SM, Lee JJ (2015). Second-generation  
490 PLINK: rising to the challenge of larger and richer datasets. *GigaScience* 4:7.  
491

492 DeGiorgio M, Rosenberg NA (2009). An unbiased estimator of gene diversity in samples containing  
493 related individuals. *Mol Biol Evol* 26:501-512.  
494

495 Gazal S, Sahbatou M, Perdry H, Letort S, Génin E, Leutenegger A (2014). Inbreeding coefficient  
496 estimation with dense SNP data: Comparison of strategies and application to HapMap III.  
497 *Hum Hered* 77:49-62.  
498

499 Gazal S, Sahbatou M, Barbron M-C, Génin E, Leutenegger A (2015). High level of inbreeding in  
500 final phase of 1000 Genomes Project. *Sci Reports* 5:17453.  
501

502 Gibson J, Morton NE, Collins A (2006). Extended tracts of homozygosity in outbred human  
503 populations, *Hum Mol Genet* 15:789-795.  
504

505 Goudet J (2005). HIERFSTAT, a package for R to compute and test hierarchical F-statistics. *Mol  
506 Ecol Notes* 5:184-186.  
507

508 Goudet J, Kay T, Weir BS (2018). How to estimate kinship. *Mol Ecol* 27:4121-4135.  
509

510 Hall N, Mercer L, Phillips D, Shaw J, Anderson AD (2012). Maximum likelihood estimation of  
511 individual inbreeding coefficients and null allele frequencies. *Genet Res* 94:151-161.  
512

513 Hill WG, Weir BS (2011). Variation in actual relationship as a consequence of Mendelian sampling  
514 and linkage. *Genet Res* 93:47-74.  
515

516 Hedrick PW (2000). *Genetics of Populations*, Second Edition. Jones and Bartlett, Sudbury, MA.  
517

518 Joshi PK, et al. (2015). Directional dominance on stature and cognition in diverse populations.  
519 *Nature* 523:459-462.  
520

521 Kardos M, Nietlisbach P, Hedrick PW (2018). How should we compare different genomic estimates  
522 of the strength of inbreeding depression? *Proc Natl Acad Sci USA* 115:E2492-E2493.  
523

524 Kelleher J, Etheridge AM, McVean G (2016). Efficient coalescent simulation and genealogical  
525 analysis for large sample sizes. *PLoS Comput Biol* 12: e1004842.  
526

527 Li CC, Horvitz DG (1953). Some methods of estimating the inbreeding coefficient. *Am J Hum*  
528 *Genet* 5:107-117.  
529

530 Malécot G (1948), *The Mathematics of Heredity*. Translated by Yermanos DM (1960). Freeman,  
531 San Francisco.  
532

533 McPeck MS, Wu X, Ober C (2004). Best linear unbiased allele-frequency estimation in complex  
534 pedigrees. *Biometrics* 60:359-367.  
535

536 Meyermans R, Gorssen W, Buys N, Janssens S (2020). How to study runs of homozygosity using  
537 PLINK? A guide for analyzing medium density SNP data in livestock and pet species. *BMC*  
538 *Genomics* 21:94.  
539

540 Narasimhan V, Danecek P, Scally A, Xue Y, Tyler-Smith C, Durbin R (2016). BCFtools/RoH:  
541 a hidden Markov model approach for detecting autozygosity from next-generation sequencing  
542 data. *Bioinformatics* 32:1749-1751.  
543

544 National Research Council (1996). *The Evaluation of Forensic DNA Evidence*. National Academies  
545 Press, Washington DC.  
546

547 Neuenschwander S, Michaud F, Goudet J (2019). quantiNemo 2: a Swiss knife to simulate complex  
548 demographic and genetic scenarios, forward and backward in time. *Bioinformatics* 35:886-888.  
549

550 Ochoa A, Storey JD (2019). FST and kinship for arbitrary population structures II: Method of  
551 moments estimators. bioRxiv (10.1101/083923) 2019. <https://doi.org/10.1101/083923>. First  
552 published 2016-10-27.  
553

554 Purcell S, Neale B, Todd-Brown K, Thomas L, Ferreira M, Bender D, Maller J, Sklar P, de Bakker  
555 P, Daly M, Sham P (2007). Plink: a toolset for whole-genome association and population-based  
556 linkage analysis. *Am J Hum Genet* 81:559-575.  
557

558 Ritland K (1996). Estimators for pairwise relatedness and individual inbreeding coefficients. *Genet*  
559 *Res Camb* 67:175-185.  
560

561 Robertson A, Hill WG (1984). Deviations from Hardy-Weinberg proportions: sampling variances  
562 and use in estimation of inbreeding coefficients. *Genetics* 107:703-718.  
563

564 Speed D, Hemani G, Johnson MR, Balding DJ (2012). Improved heritability estimation from  
565 genome-wide SNPs. *Am J Hum Genet* 91:1011-1021.  
566

567 Steele CD, Syndercombe Court D, Balding DJ (2014). Worldwide  $F_{ST}$  estimates relative to five  
568 continental-scale populations. *Ann Hum Genet* 78:468-477.

569 The 1000 Genomes Project Consortium (2015). A global reference for human genetic variation.  
570 *Nature* 526:68-87.  
571

572 VanRaden PM (2008) Efficient methods to compute genomic predictions. *J Dairy Sci* 91:4414-4423.  
573

574 Vogl C, Karhu A, Moran G, Savolainen O (2002). High resolution analysis of mating systems:  
575 inbreeding in natural populations of *Pinus radiata*. *J Evol Biol* 15:433-439.  
576

577 Wang J (2016). Pedigrees or markers: Which are better in estimating relatedness and inbreeding  
578 coefficient? *Theoret Pop Biol* 107:4-13.  
579

580 Weir BS (1996). *Genetic Data Analysis II*. Sinauer, Sunderland, MA.  
581

582 Weir BS, Cockerham CC (1984). Estimating F-statistics for the analysis of population structure.  
583 *Evolution* 38:1358-1370.  
584

585 Weir BS, Goudet J (2017). A unified characterization for population structure and relatedness.  
586 *Genetics* 206:2085-2103.  
587

588 Weir BS, Hill WG (2002). Estimating F-statistics. *Ann Rev Genet* 36:721-750.  
589

- 590 Wright S (1922). Coefficients of inbreeding and relationship. *Am Naturalist* 56:330-338.  
591
- 592 Yang J, Lee SH, Goddard ME, Visscher PM (2011). GCTA: A tool for genome-wide complex trait  
593 analysis. *Am J Hum Genet* 88:76-82.  
594
- 595 Yengo L, Zhu Z, Wray NR, Weir BS, Yang J, Robinson MR, Visscher PM (2017). Detection and  
596 quantification of inbreeding depression for complex traits from SNP data. *Proc Natl Acad Sci*  
597 *USA* 114:8602-8607.  
598
- 599 Yengo L, Zhu Z, Wray NR, Weir BS, Yang J, Robinson MR, Visscher PM (2018). Estimation of  
600 inbreeding depression from SNP data REPLY. *Proc Natl Acad Sci USA* 115:E2494-E2495.  
601
- 602 Zheng X, Levine D, Shen J, Gogarten S, Laurie C, Weir B (2012). A high-performance computing  
603 toolset for relatedness and principal component analysis of SNP data. *Bioinformatics* 28: 3326-  
604 3328.

**Table 1:** Measures of Inbreeding and Coancestry.

Measure	Description	Evaluation
$F_j$	Inbreeding coefficient for individual $j$ : ibd probability for homologous alleles	$F_{\text{PED}}$ : Path counting. $F_{\text{Gold}}$ : Actual ibd in simulations.
$\theta_{jj'}$	Coancestry for individuals $j, j'$ : ibd probability for random alleles from $j$ and $j'$ .	$F_{\text{PED}}$ : Path counting. $F_{\text{Gold}}$ : Actual ibd in simulations.
The following hold for PED and Gold values.		
$F_W$	Average inbreeding coefficient.	$F_W = \frac{1}{n} \sum_{j=1}^n F_j$ for $n$ individuals.
$\Psi_j$	Average coancestry coefficient for individual $j$ .	$\Psi_j = \frac{1}{n-1} \sum_{j'=1, j' \neq j}^n \theta_{jj'}$
$\theta_S$	Average coancestry coefficient.	$\theta_S = \frac{1}{n} \sum_{j=1}^n \Psi_j$
$f_j$	Within-population inbreeding coefficient for individual $j$ .	$f_j = \frac{F_j - \theta_S}{1 - \theta_S}$
$f_W$	Average within-population inbreeding coefficient.	$f_W = \frac{F_W - \theta_S}{1 - \theta_S}$
$\psi_j$	Within-population average kinship coefficient for individual $j$ .	$\psi_j = \frac{\Psi_j - \theta_S}{1 - \theta_S}$



**Table 2:** Estimators of Inbreeding.

Estimate	Calculation*	Expected Value†
$\hat{F}_{\text{ROH}_j}$	Proportion of homozygous blocks.	No explicit expression.
$\hat{F}_{\text{MLE}_j}$	Maximization of likelihood for $f_j$ .	No explicit expression.
$\hat{F}_{\text{HOM}_j}$	$1 - \frac{\sum_l X_{jl}(2 - X_{jl})}{\sum_l 2\tilde{p}_l(1 - \tilde{p}_l)}$	$\frac{f_j - \frac{1}{2n}(1 + f_W)}{1 - \frac{1}{2n}(1 + f_W)}$
$\hat{F}_{\text{HOM}_W}$	$1 - \frac{1}{n} \sum_{j=1}^n \frac{\sum_l X_{jl}(2 - X_{jl})}{\sum_l 2\tilde{p}_l(1 - \tilde{p}_l)}$	$\frac{f_W - \frac{1}{2n}(1 + f_W)}{1 - \frac{1}{2n}(1 + f_W)}$
$\hat{F}_{\text{AS}_j}$	$\frac{\sum_l (\tilde{A}_{jl} - \tilde{A}_{Sl})}{\sum_l (1 - \tilde{A}_{Sl})}$	$f_j$
$\hat{F}_{\text{AS}_W}$	$\frac{1}{n} \sum_{j=1}^n \hat{F}_{\text{AS}_j}$	$f_W$
$\hat{F}_{\text{UNI}_j}^w$	$\frac{\sum_l [X_{jl}^2 - (1 + 2\tilde{p}_l)X_{jl} + 2\tilde{p}_l^2]}{\sum_l 2\tilde{p}_l(1 - \tilde{p}_l)}$	$\frac{f_j - 2\psi_j - \frac{1}{2n}(3 + 4f_j - 8\psi_j - f_W)}{1 - \frac{1}{2n}(1 + f_W)}$
$\hat{F}_{\text{UNI}_W}^w$	$\frac{1}{n} \sum_{j=1}^n \hat{F}_{\text{UNI}_j}^w$	$\frac{f_W - \frac{3}{2n}(1 + f_W)}{1 - \frac{1}{2n}(1 + f_W)}$
$\hat{F}_{\text{UNI}_j}^u$	$\frac{1}{L} \sum_{l=1}^L \frac{X_{jl}^2 - (1 + 2\tilde{p}_l)X_{jl} + 2\tilde{p}_l^2}{2\tilde{p}_l(1 - \tilde{p}_l)}$	No explicit expression.
$\hat{F}_{\text{STD}_j}^w$	$\frac{\sum_l (X_{jl} - 2\tilde{p}_l)^2}{\sum_l 2\tilde{p}_l(1 - \tilde{p}_l)} - 1$	$\frac{f_j - 4\psi_j - \frac{1}{2n}(3 + 4f_j - 8\psi_j - f_W)}{1 - \frac{1}{2n}(1 + f_W)}$
$\hat{F}_{\text{STD}_W}^w$	$\frac{1}{n} \sum_{j=1}^n \hat{F}_{\text{STD}_j}^w$	$\frac{f_W - \frac{3}{2n}(1 + f_W)}{1 - \frac{1}{2n}(1 + f_W)}$
$\hat{F}_{\text{STD}_j}^u$	$\frac{1}{L} \sum_{l=1}^L \frac{(X_{jl} - 2\tilde{p}_l)^2}{2\tilde{p}_l(1 - \tilde{p}_l)} - 1$	No explicit expression.

\*  $X_{jl}$  is the reference allele dosage for SNP  $l$  in individual  $j$ .

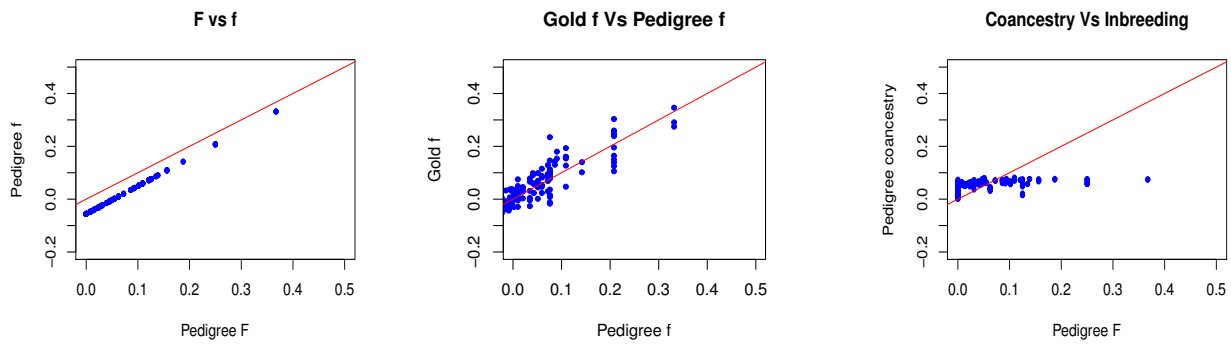
\*  $\tilde{p}_l = \frac{1}{2n} \sum_{j=1}^n X_{jl}$  is the sample allele frequency for SNP  $l$ .

† For weighted averages over large numbers of loci.

**Table 3:** Correlations among inbreeding measures\* for simulated data.

	$F_{\text{PED}}$	$F_{\text{Gold}}$	$\hat{F}_{\text{ROH}}$	$f_{\text{PED}}$	$f_{\text{Gold}}$	$\hat{f}_{\text{AS}}$	$\hat{f}_{\text{HOM}}$	$\hat{f}_{\text{MLE}}$	$f_{\text{UNI}}^{\text{Gold}}$	$\hat{f}_{\text{UNI}}^{\text{w}}$	$\hat{f}_{\text{UNI}}^{\text{u}}$	$f_{\text{STD}}^{\text{Gold}}$	$\hat{f}_{\text{STD}}^{\text{w}}$	$\hat{f}_{\text{STD}}^{\text{u}}$
$F_{\text{PED}}$	1.00	0.94	0.92	1.00	0.94	0.84	0.84	0.80	0.80	0.71	0.74	0.44	0.36	-0.25
$F_{\text{Gold}}$	0.94	1.00	0.99	0.94	1.00	0.90	0.90	0.88	0.86	0.78	0.80	0.48	0.41	-0.24
$\hat{F}_{\text{ROH}}$	0.92	0.99	1.00	0.92	0.99	0.91	0.91	0.89	0.87	0.80	0.82	0.50	0.45	-0.20
$f_{\text{PED}}$	1.00	0.94	0.92	1.00	0.94	0.84	0.84	0.80	0.80	0.71	0.74	0.44	0.36	-0.25
$f_{\text{Gold}}$	0.94	1.00	0.99	0.94	1.00	0.90	0.90	0.88	0.86	0.78	0.80	0.48	0.41	-0.24
$\hat{f}_{\text{AS}}$	0.84	0.90	0.91	0.84	0.90	1.00	1.00	0.99	0.77	0.86	0.86	0.42	0.44	-0.22
$\hat{f}_{\text{HOM}}$	0.84	0.90	0.91	0.84	0.90	1.00	1.00	0.99	0.77	0.86	0.86	0.42	0.44	-0.22
$\hat{f}_{\text{MLE}}$	0.80	0.88	0.89	0.80	0.88	0.99	0.99	1.00	0.82	0.92	0.91	0.53	0.57	-0.10
$f_{\text{UNI}}^{\text{Gold}}$	0.80	0.86	0.87	0.80	0.86	0.77	0.77	0.82	1.00	0.89	0.91	0.86	0.74	0.18
$\hat{f}_{\text{UNI}}^{\text{w}}$	0.71	0.78	0.80	0.71	0.78	0.86	0.86	0.92	0.89	1.00	0.98	0.75	0.84	0.17
$\hat{f}_{\text{UNI}}^{\text{u}}$	0.74	0.80	0.82	0.74	0.80	0.86	0.86	0.91	0.91	0.98	1.00	0.76	0.80	0.17
$f_{\text{STD}}^{\text{Gold}}$	0.44	0.48	0.50	0.44	0.48	0.42	0.42	0.53	0.86	0.75	0.76	1.00	0.87	0.55
$\hat{f}_{\text{STD}}^{\text{w}}$	0.36	0.41	0.45	0.36	0.41	0.44	0.44	0.57	0.74	0.84	0.80	0.87	1.00	0.53
$\hat{f}_{\text{STD}}^{\text{u}}$	-0.25	-0.24	-0.20	-0.25	-0.24	-0.22	-0.22	-0.10	0.18	0.17	0.17	0.55	0.53	1.00

\* As shown in Tables 1 and 2.



Pedigree  $f$  vs Pedigree  $F$

Gold  $f$  vs Pedigree  $f$

Pedigree coancestry vs Pedigree  $f$

**Figure 1:** Allele sharing estimates for 283 non-founders in simulated pedigree.

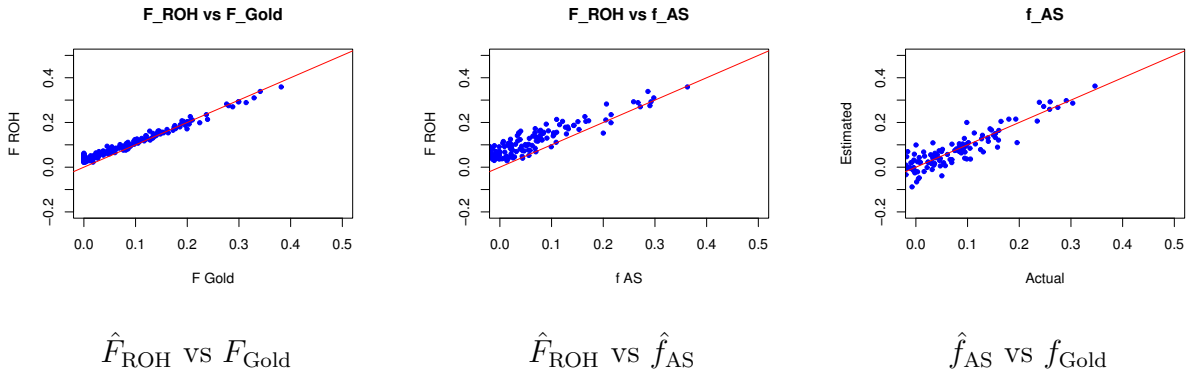
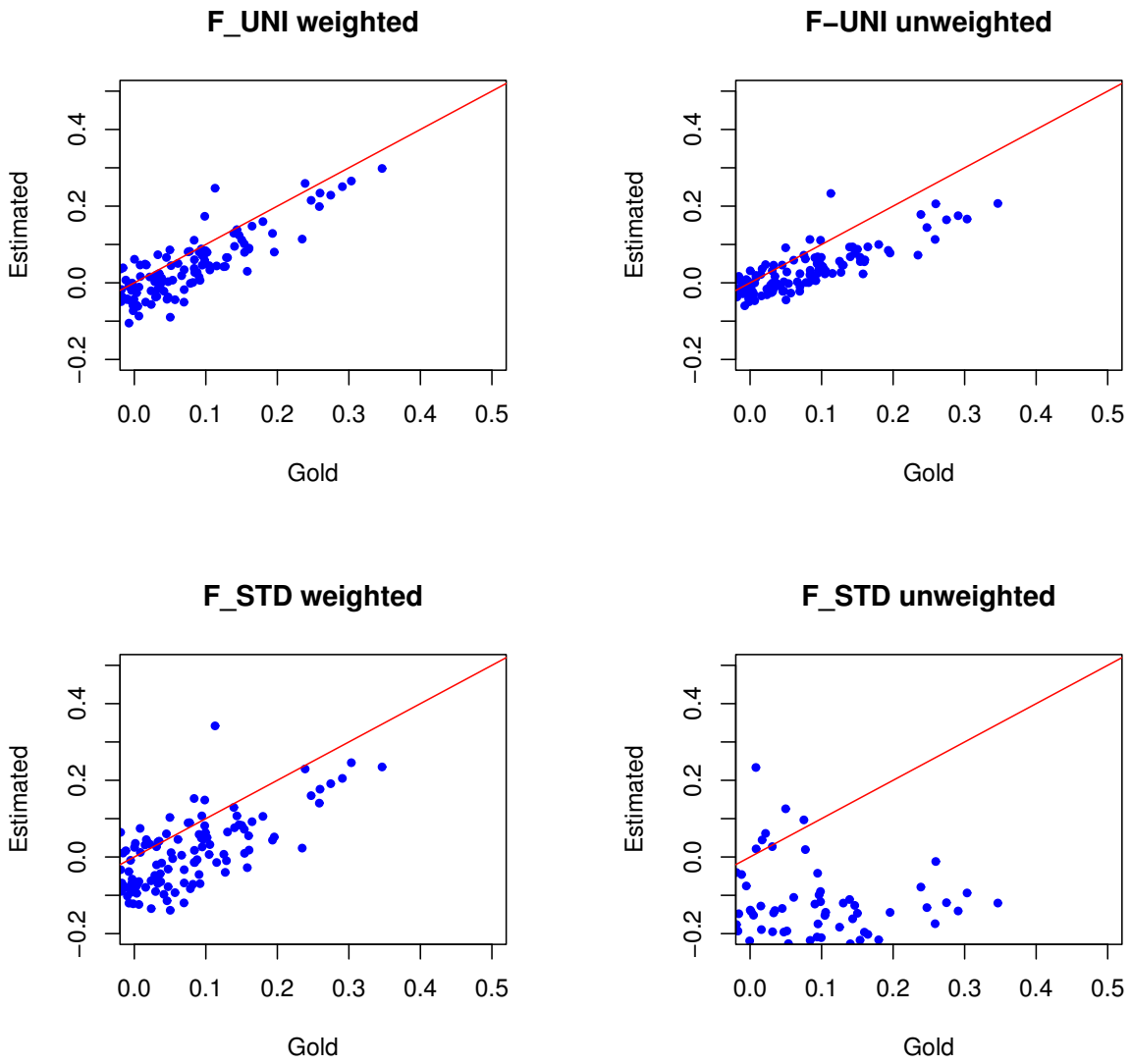


**Figure 2:** Values of ROH estimates of  $F$  and allele-sharing estimates of  $f$  for 283 non-founders in simulated pedigree.



Weighted  $\hat{f}_{\text{UNI}}$  and  $\hat{f}_{\text{STD}}$  vs  $f_{\text{Gold}_j}$

Unweighted  $\hat{f}_{\text{UNI}}$  and  $\hat{f}_{\text{STD}}$  vs  $f_{\text{Gold}_j}$

**Figure 3:** Values of UNI and STD estimates for 283 non-founders in simulated pedigree.

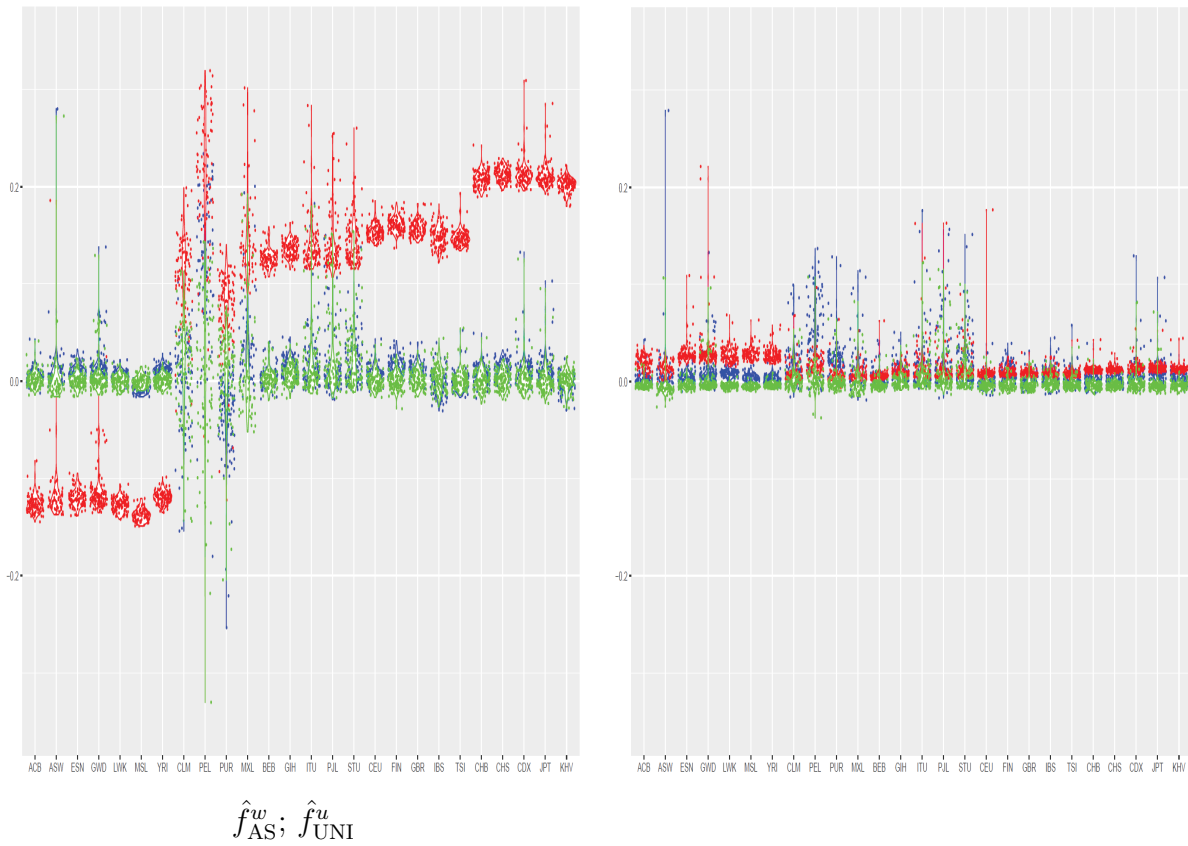


**Figure 4:** Individual inbreeding coefficient estimates for 1000 Genomes data.

Green: Population as reference; Blue: Continental group as reference; Red: World as reference.

Populations (left to right): ACB, ASW, ESN, GWD, LWK, MSL, YRI (AFR); CLM, MXL, PEL, PUR (AMR); CDX, CHB, CHS, JPT, KHV (EAS); CEU, FIN, GBR, IBS, TSI (EUR); BEB, GIH, ITU, PUL, STR (SAS).

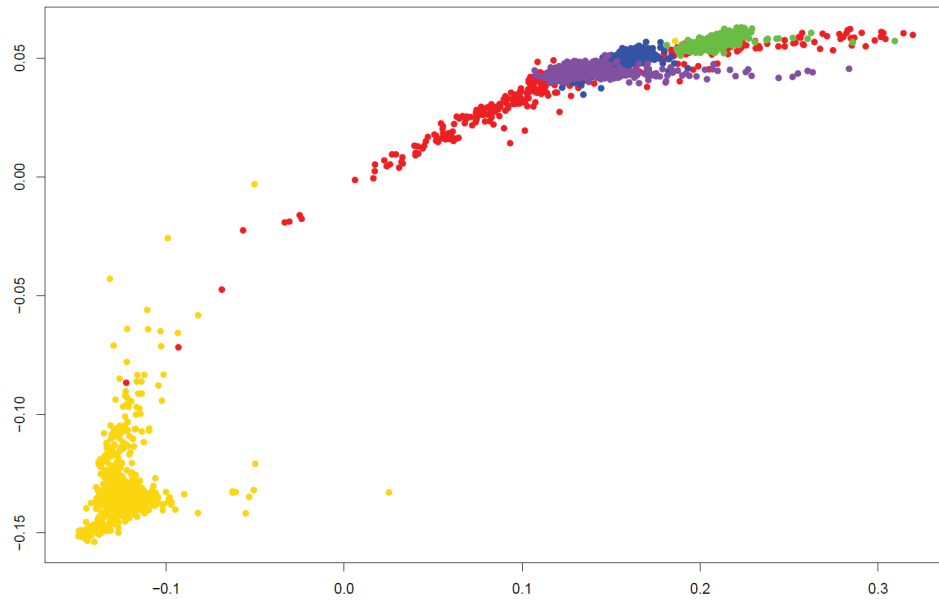


**Figure 5:** Estimates  $\hat{\psi}_{AS_j}$  of within-population individual-specific average kinships (Y-axis) vs estimates  $\hat{f}_{AS_j}$  of within-population individual-specific inbreeding coefficients (X-axis) for 1000 Genomes data, with the World as reference set. Gold: AFR; Red: AMR; Purple: SAS; Blue: EUR; Green: EAS.

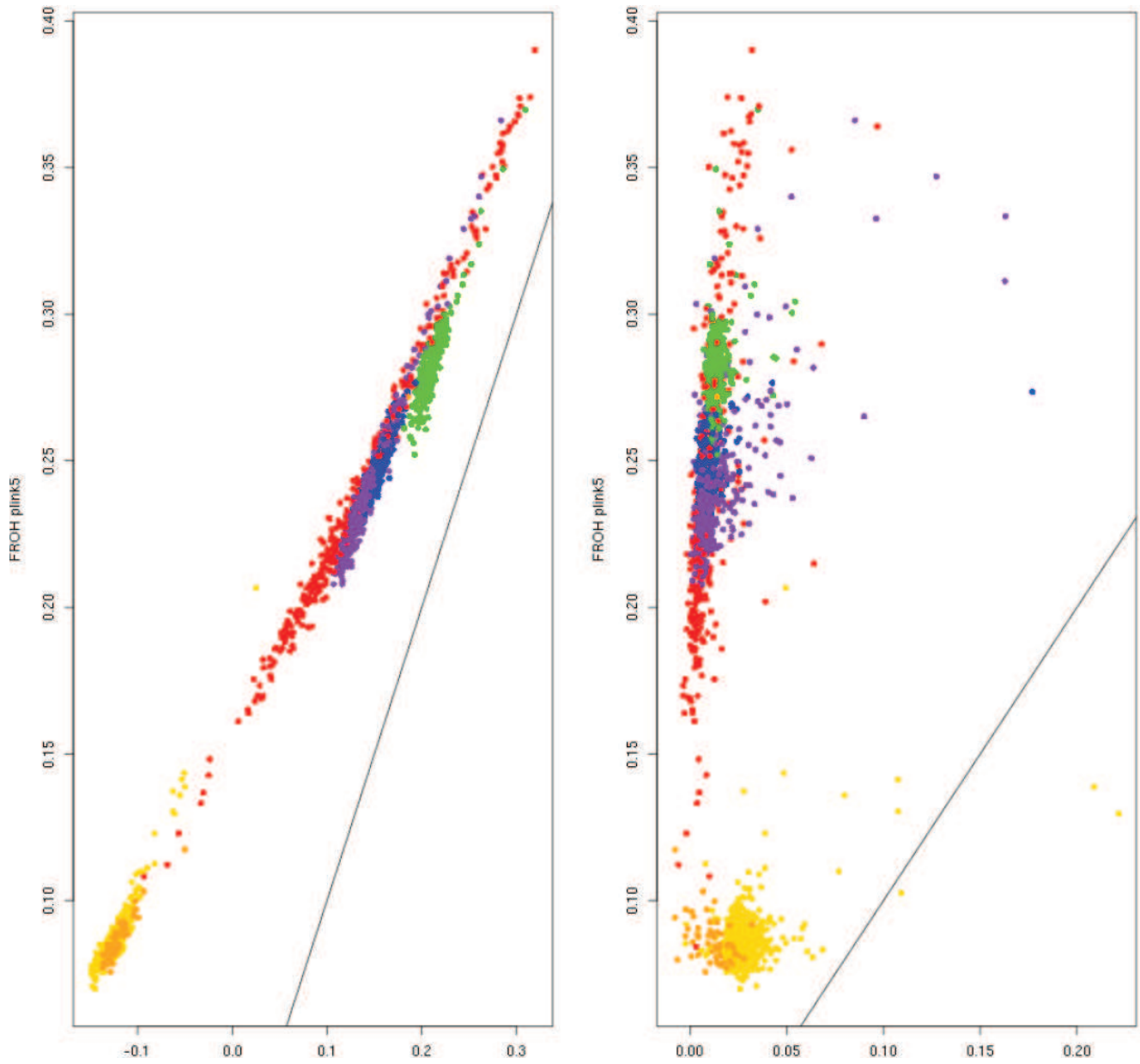


**Figure 6:** PLINK-estimates  $\hat{f}_{\text{ROH}}$  (Y-axis) vs SNP by SNP estimates for 1000 Genomes data, with the World as a reference set. Left Panel:  $\hat{f}_{\text{AS}}^w$  (X-axis) ; Right panel:  $\hat{f}_{\text{UNI}}^u$  (X-axis). Solid line  $X = Y$  in both panels. Gold: AFR, not ACB, ASW; Orange: AFR, ACB and ASW; Red: AMR; Purple: SAS; Blue: EUR; Green: EAS.



## Supplementary Figure S1: 1000 Genomes Estimates

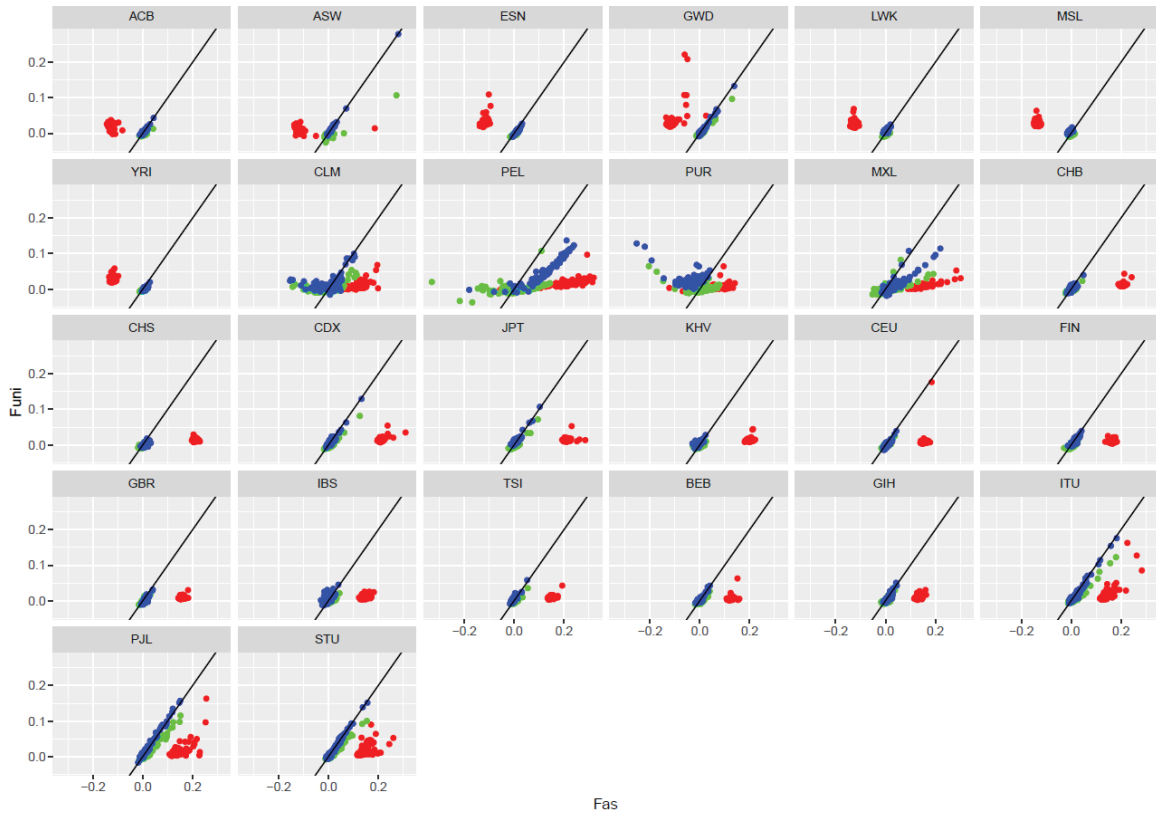


**Figure S1:** Values of  $\hat{f}_{\text{UNI}}$  (Y-axis) versus  $\hat{f}_{\text{AS}}$  (X-axis) for the 1000 Genomes populations. Population reference in green, continental reference in blue, world reference in red.

# Supplementary Figure S2: 1000 Genomes Estimate Ranks

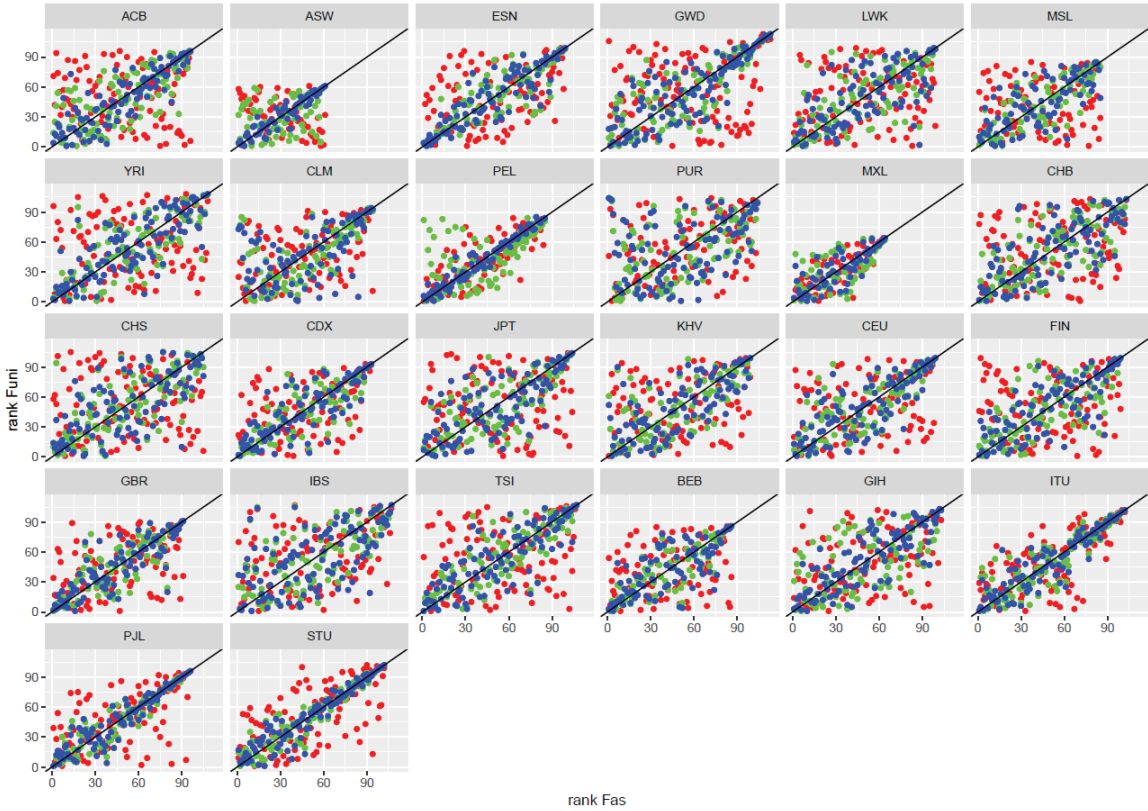


**Figure S2:** Ranks of  $\hat{f}_{UNI}$  (Y-axis) versus ranks of  $\hat{f}_{AS}$  (X-axis) for the 1000 Genomes populations. Population reference in green, continental reference in blue, world reference in red.

## Supplementary Figure S3:

Use of Continent vs World Allele Frequencies.

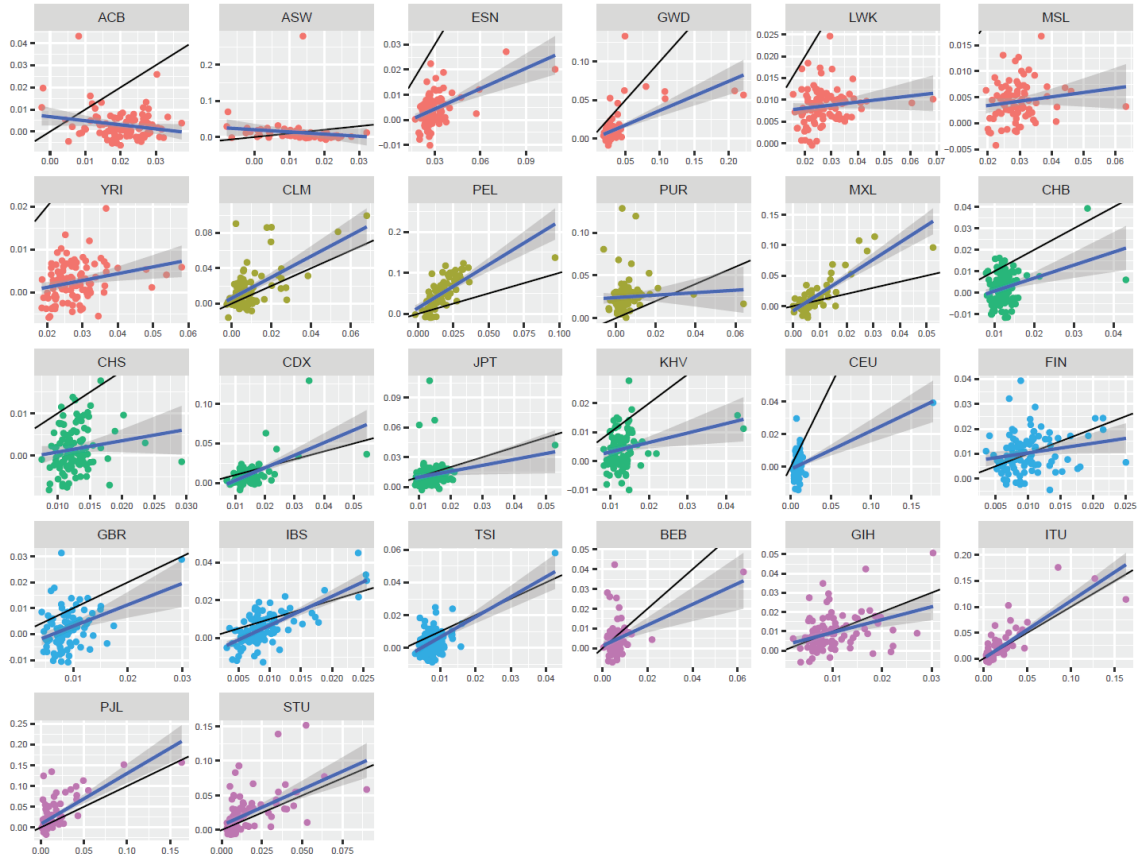


**Figure S3:** Values of  $\hat{f}_{\text{UNI}}$  for each of the 1000 Genomes populations with the continent for that population providing the sample allele frequencies (Y axis) versus the world providing the sample allele frequencies (X axis). Red: AFR; Gold: AMR; Green: SAS; Blue: EUR; Purple: SAS.

## Supplementary Figure S4:

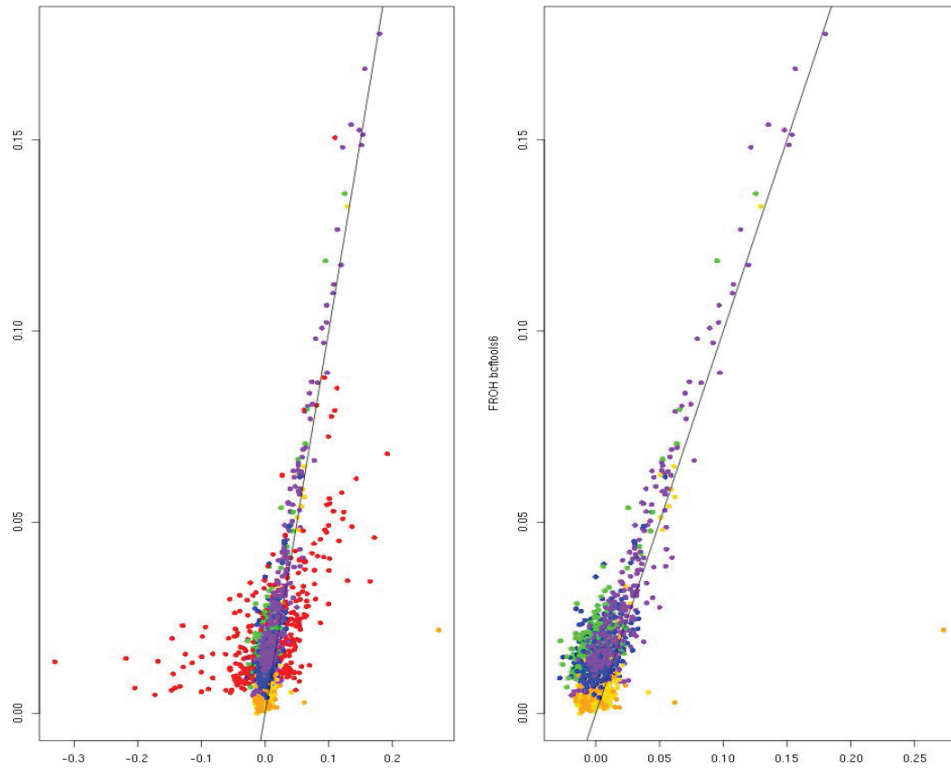


**Figure S4:** BCF-tools-estimates  $\hat{f}_{\text{BCF}}$  (Y-axis) vs  $\hat{f}_{\text{AS}}^w$  (X-axis) for 1000 Genomes data, with the Population as a reference set. Left Panel: All 1000 Genomes populations; Right panel: Omitting AMR populations. Solid line  $X = Y$  in both panels. Gold: AFR, not ACB, ASW; Orange: AFR, ACB and ASW; Red: AMR; Purple: SAS; Blue: EUR; Green: EAS.

## Supplementary Figure S5:

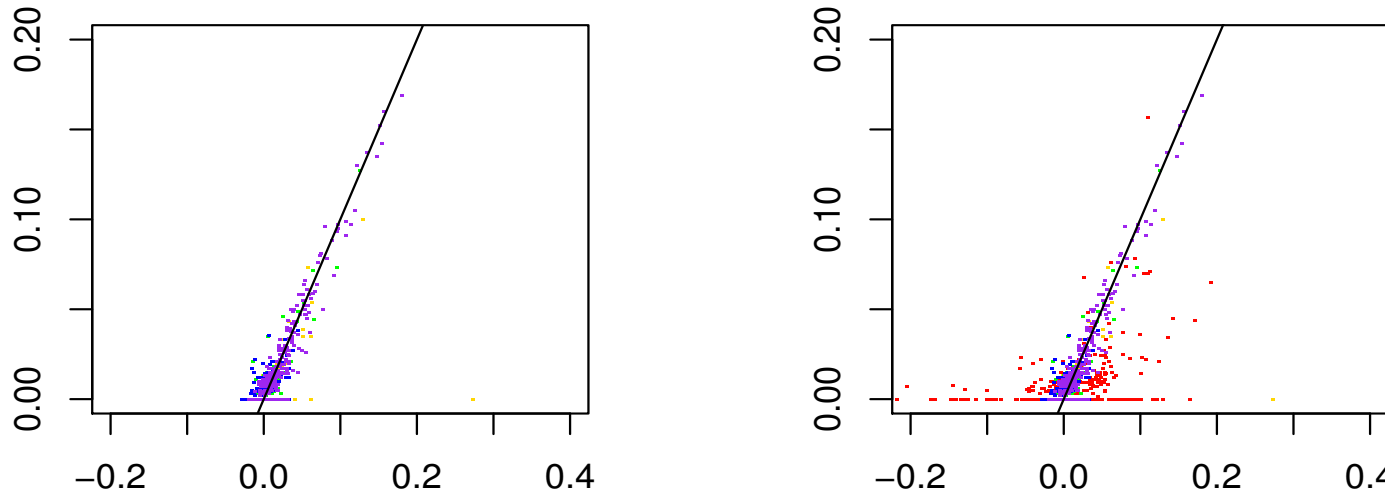


**Figure S5:** Fsuite estimates  $\hat{f}_{Fsuite}$  (Y-axis) vs  $\hat{f}_{AS}^w$  (X-axis) for 1000 Genomes data, with the Population as a reference set. Left Panel: All 1000 Genomes populations; Right panel: Omitting AMR populations. Solid line  $X = Y$  in both panels. Gold: AFR; Red: AMR; Purple: SAS; Blue: EUR; Green: EAS.